Yield stress determines bioprintability of hydrogels based on gelatin-methacryloyl and gellan gum for cartilage bioprinting

Yield stress determines bioprintability of hydrogels based on gelatin-methacryloyl and gellan gum for cartilage bioprinting

Vivian H. M. Mouser[1], Ferry P.W. Melchels[1,2], Jetze Visser[1], Wouter J.A. Dhert[3], Debby Gawlitta[4], Jos Malda[1,5]

[1] Department of Orthopaedics, University Medical Center Utrecht, PO box 85500, 3508 GA Utrecht, the Netherlands

[2] Institute of Biological Chemistry, Biophysics and Bioengineering, School of Engineering and Physical Sciences, Heriot-Watt University, Edinburgh, United Kingdom

[3] Faculty of Veterinary Medicine, Utrecht, the Netherlands

[4] Department of Oral and Maxillofacial Surgery & Special Dental Care, University Medical Center Utrecht, Utrecht, the Netherlands

[5] Department of Equine Sciences, Faculty of Veterinary Medicine, Utrecht, the Netherlands

1. Abstract

Bioprinting of chondrocyte-laden hydrogels facilitates the fabrication of constructs with controlled organization and shape for *e.g.* articular cartilage implants. Gelatin-methacryloyl (gelMA) supplemented with gellan gum is a promising bio-ink. However, the rheological properties governing the printing process, and the influence of gellan gum on the mechanical properties and chondrogenesis of the blend, are still unknown. Here, we investigated the suitability of gelMA/gellan for cartilage bioprinting.

Multiple concentrations, ranging from 3-25% gelMA with 0-1.5% gellan gum, were evaluated for their printability, defined as the ability to form filaments and to incorporate cells at 15-37°C. To support the printability assessment, yield stress and viscosity of the hydrogels were measured. Stiffness of UV-cured constructs, as well as cartilage-like tissue formation by embedded chondrocytes, were determined *in vitro*.

A large range of gelMA/gellan concentrations were printable with inclusion of cells and formed the bioprinting window. Addition of gellan gum improved filament deposition by inducing yielding behavior, increased construct stiffness, and supported chondrogenesis. High gellan gum concentrations, however, did compromise cartilage matrix production and distribution, and even higher concentrations resulted in too high yield stresses to allow cell encapsulation.

This study demonstrates the high potential of gelMA/gellan blends for cartilage bioprinting and identifies yield stress as dominant factor for bioprintability.

2. Introduction

Additive manufacturing techniques *e.g.* bioprinting, melt electrospinning, and stereolithography, allow the fabrication of organized three dimensional (3D) constructs to regenerated or replace damaged tissues[1–3]. Especially, bioprinting is a promising technique to create such tissue engineered constructs, as it allows accurate positioning of cells and biomaterials in a layered fashion[1,4]. As a result, constructs with controlled porosity to provide optimal diffusion of nutrients, oxygen, and waste products for embedded cells can be fabricated.

Bioprinting techniques are rapidly advancing, yet, the search for suitable bioprinting materials, the so-called 'bio-inks', remains challenging[2,5]. Multiple physicochemical material properties that are favorable for printing have been identified *e.g.* fast gelation after extrusion (thermo-gelation and/or cross-linking), high viscosity, yielding behavior, and shear thinning[4,6]. However, it is not clear what the most dominant properties are and in what range these parameters should be to ensure printing with high shape-fidelity. Additionally, a bio-ink should allow the incorporation of cells and should have biological properties to support cell survival, differentiation, and tissue formation.

Hydrogels seem to be the most promising basis for bio-inks, as they can mimic the natural cell habitat and have a high water content, which supports cell survival and facilitates a homogeneous cell distribution inside the 3D structure. Additionally, hydrogels allow the formation of constructs with various shapes and mechanical properties, and relevant biological and chemical cues can be easily incorporated. Nonetheless, it is difficult to unite the appropriate physicochemical and biological material properties in one hydrogel system. Highly viscous hydrogels with high cross-linking densities are favorable to fabricate constructs with high shape-fidelity. Contrarily, liquid hydrogels with low crosslinking densities are more favorable for the differentiation of cells[7,8].

Several hydrogel systems have been explored for their potential as a bio-ink, including hydrogels based on collagen[9], gelatin[10–12], hyaluronic acid[13], chitosan[14], alginate[15], poly(ethylene glycol)[16], hydroxyethyl-methacrylate-derivatized dextran[17], and poly(N-hydroxypropyl-methacrylacrylamide lactate)[18]. Of these, gelatin has great potential for bioprinting as it exhibits thermo-gelation to support the printing process and it contains inherent cell adhesion domains, low immunogenicity, and can be degraded enzymatically to support cells in their tissue formation[19,20]. Furthermore, gelatin can be functionalized with methacrylamide and (to a lesser extent) methacrylate groups to enable cross-linking with UV light, which can permanently fix the shape of a printed construct and thus generates mechanical stability[21].

Important targets for the implantation of 3D printed, tissue engineered constructs, are articular cartilage defects. As, articular cartilage lacks vasculature and innervation, and contains only few chondrocytes, it has low self-renewal capacity[22,23]. Additionally, bioprinting provides the opportunity

to replicate the zonal organization of articular cartilage, by combining multiple biomaterials and/or cells in a single construct[11,24]. Recent studies have shown that gelatin-methacryloyl (gelMA) supports cartilage-like tissue formation of both mesenchymal stem cells and chondrocytes *in vitro*[10,25–27]. Hence, gelMA-based hydrogels are extremely interesting for the treatment of cartilage defects.

The suitability of gelMA as a bio-ink for the printing of 3D structures has also been demonstrated[12]. However, printing gelMA on its own requires relatively high polymer concentrations, ultra-precise control of ink and nozzle temperatures, and cooling of the building platform, as gelMA has low viscosity and relatively slow thermal gelation[12].

Recently, Melchels et al. (2014)[28] demonstrated that the addition of gellan gum to a gelMA hydrogel can significantly increase the viscosity and speed of gelation of the hydrogel blend. This effect is due to the ionic cross-links that gellan gum can form with gelMA and itself, which induces pseudo-plasticity (a form of shear thinning) and yield stress[28]. Additionally, gellan gum is known to support the chondrogenic potential of mesenchymal stem cells and chondrocytes *in vivo*[29].

The demonstration of the beneficial effect of gellan gum on the printablity of gelMA is a promising step forward for the 3D bioprinting of gelMA-based cartilage repair constructs. However, further evaluation is essential as this effect was only demonstrated for one gelMA/gellan concentration. Additionally, the influence of gellan gum on the mechanical properties of the UV cross-linked blends and on the chondrogenic potential of embedded cells is yet unknown. Therefore, the aim of this study is to relate different concentrations and ratios of gelMA/gellan to the hydrogel's printability (filament formation and deposition), mechanical properties, and chondrogenic potential. We expect not only to find the optimal compositions for cartilage bioprinting, but also to identify the rheological property or properties that dictate bioprinting behavior. Consequently, this paper reveals the cartilage bioprinting window for gelMA/gellan blends.

3. Materials and Methods

3.1. Preparation of polymer solution

GelMA was synthesized by reacting gelatin (Sigma Aldrich, type A from porcine skin, 175g Bloom; Zwijndrecht, the Netherlands) with methacrylic anhydride (Sigma Aldrich) as previously described[28]. The polymer was freeze-dried and stored at -20°C until further use.

Irgacure 2959 (gift from BASF, Ludwigshafen, Germany) was dissolved in MilliQ with 10% PBS v/v (optimal salt concentration for the ionic interaction of gelMA with gellan gum[28]) at 70°C for 20 minutes, to a final concentration of 0.1% w/v. To generate an isotonic solution, 4.86% D-(+)-mannose (Sigma Aldrich) was added. The solution was filter-sterilized and used to dissolve gelMA and low-acyl gellan gum (Gelzan™ CM, Gelrite®; Sigma Aldrich) at different concentrations, as shown in Figure 1.

3.2. Screening of filament formation

Multiple polymer concentrations and ratios (Figure 1) were prepared, aspirated in a 3 ml Luer Lock syringe with a 23 gauge metal needle (Precision Tip PN 7018302, Nordson EFD, Bedfordshire, England), and loaded into the BioScaffolder dispensing system (SYS+ENG, Salzgitter-Bad, Germany). The BioScaffolder fabricates 3D structures by coordinated motion of, in this case, a piston-driven dispensing head while depositing on a stationary platform. The syringe temperature was varied from 37°C to 15°C in the dispensing head and the ability to deposit a filament was evaluated. First, the shape of the polymer solution at the nozzle was observed. When a droplet formed, as described by Schuurman *et al.* (2013)[10], the print temperature was considered too high and would be reduced until a continuous filament was formed at the nozzle. When a filament could be formed, *Π*-shaped lines were printed. A polymer solution was considered printable if a *Π*-shape could be printed without corrugation, droplet formation or interruptions in the final structure. If corrugations occurred the printing temperature was considered too low and if droplets formed the printing temperature was considered too high (Figure 2). Images of the deposited filaments were made with a stereomicroscope (Olympus SZ61, SZ2-ILST, Olympus DP70 camera, Hamburg, Germany). Furthermore, the possibility to mix cell into the polymer solution using a gel pipette was assessed at 37°C. The mixing was considered successful if the cells were completely resuspended and no air bubbles or lumps appeared in the cell-laden polymer solution.
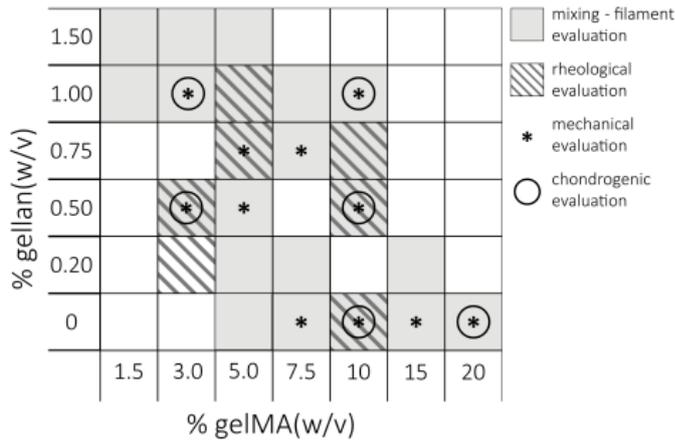
Fig. 1. A schematic overview of all evaluated gelMA/gellan concentrations. Hydrogel formulations were evaluated for their printability and the ability to mix them with a cell pellet at 37°C (grey), rheological properties (hatched grey), mechanical properties after UV cross-linking (*), and for cartilage-like tissue formation of embedded chondrocytes (○).
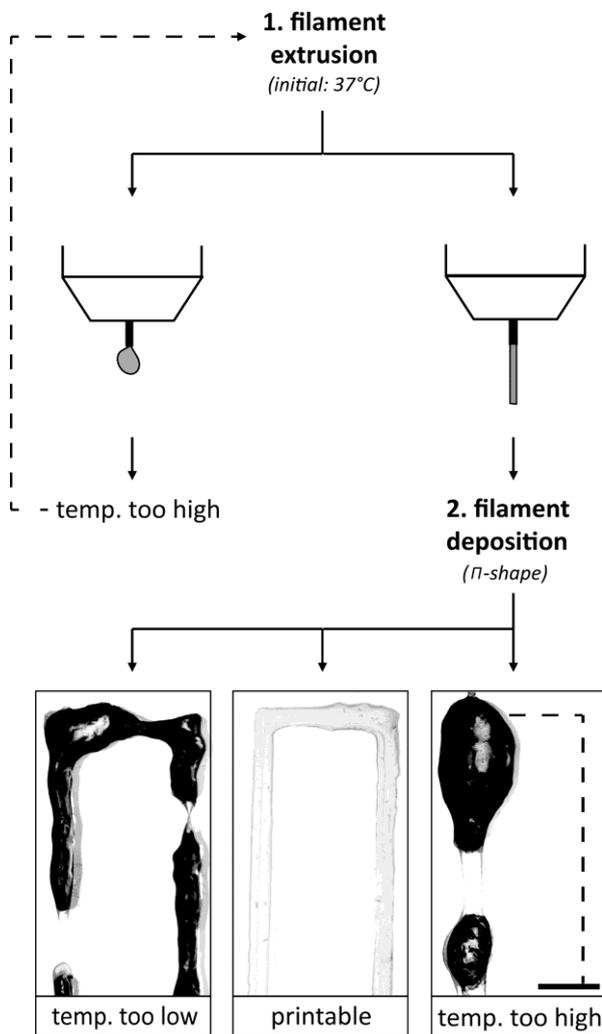
Fig. 2. A schematic overview of the iterative hydrogel filament screening process. First filament extrusion was evaluated (1), when the temperature was too high (droplet formation) it was lowered and evaluated again, and when a certain temperature allowed filament extrusion, the appearance of the deposited filament was evaluated by printing a Π-shape (2). The print temperature was adjusted until a smooth filament was formed or until an endless loop occurred which meant that the hydrogel formulation was unprintable at a temperature of 15-37°C. The irregularities of the filament surface cause light scatter, which turns black on the pictures. Scale bar represents 2 mm and the dotted line in the printed structures represents the missing part of the Π-shape.

3.3. Rheometry

To support the filament printing observations, rheological measurements were performed on selected hydrogel compositions (Figure 1) using an AR G-2 rheometer (TA-Instruments, Etten-Leur, the Netherlands) equipped with a cone-plate geometry (cone diameter: 20 mm; angle: 1°; gap: 300 µm). For a selection of printable gels (3/0.5%; 10/0%; 10/0.5% gelMA/gellan), yield stress was measured in duplicate at the observed optimal temperatures for filament deposition (logarithmic flow ramp, loading temperature: 80°C, after loading the temperature was reduced to the measuring temperature and an additional 120 seconds was waited to ensure the whole sample contained the proper temperature, stress: 0.1-1000 Pa; duration of measurement: 5 minutes). To explore the lower boundary of the bioprinting window, the yield stress was measured at 15°C for the 3/0.2% gelMA/gellan formulation, which did not form a filament between 15°C and 37°C. To explore the upper boundary of the bioprinting window, the yield stress was measured for multiple gel formulations just below and above this boundary (5/0.75%, 5/1%, 10/0.5% and 10/0.75% gelMA/gellan) at 37°C (flow ramp, loading temperature: 80°C, when measuring temperature is reached wait 10 minutes, stress: 10-10,000 Pa; duration: 5 minutes). In addition, the viscosity of these four formulations was measured in flow in triplicate at 37°C (flow peak hold, wait for temperature, shear rate: 300/s, duration: 20 minutes). All polymer solutions were freshly prepared as described in the section 'preparation of polymer solution' before the measurements. The yield stress was defined as the stress at which the polymer solution first started to flow, indicated as the first read-out of shear rate and viscosity on the rheometer. The corresponding viscosity drop was determined by the difference in viscosity at the yield stress and at a ten times higher stress. When the graph reached a plateau before it reached a ten times higher stress, the difference between the viscosity at the yield stress and the viscosity at the plateau was reported for the viscosity drop. The hydrogel viscosity was defined as the average viscosity of the final 10 minutes of the viscosity measurement.

3.4. Construct stiffness

Cell-free samples (n = 3) were prepared by injecting the different polymer solutions (Figure 1) into custom-made cylindrical Teflon molds (diameter: 6 mm; height 2 mm). Next, samples were UV cross-linked by exposure to 365 nm UV light (2.6 mW/cm^2, UVP CL-1000) for 15 minutes. After removing the hydrogels from the molds, they were incubated in DMEM/F-12+GlutaMax-1 (Dulbecco's Modified Eagle Medium, 31331, Invitrogen, Carlsbad, California, USA) supplemented with 5% heat-inactivated fetal bovine serum (FBS, Biowhittaker, Breda, the Netherlands) and pen/strep (final concentration 100 units/ml penicillin and 100 µg/ml streptomycin, Gibco) for 24 hours at 37°C. A stress/strain curve was obtained for each hydrogel construct under unconfined compression using a

Dynamic Mechanical Analyzer (DMA, Q800 TA-Instrument) to determine the Young's modulus. The hydrogel constructs (three for each condition) were subjected to a preload force of 0.001 N and subsequently compressed with a force ramp rate of 0.5 N/min and an upper force limit of 1.5 N. The Young's modulus was calculated as the initial slope (around 2% strain) of the stress/strain curve.

3.5. Cell isolation

To obtain primary chondrocytes, full-thickness cartilage was harvested under sterile conditions from the stifle joints of fresh equine cadavers (3 donors; 3–10 years old; with consent of the owners). The horses had macroscopically healthy cartilage. Cartilage samples were digested overnight at 37°C in DMEM (61965, Invitrogen) supplemented with 0.15% collagenase type II (Worthington Biochemical Corp, Vollenhove, the Netherlands). After incubation, the suspension was filtered through a 100 μm cell strainer and the chondrocytes were washed and stored at passage 0 in liquid nitrogen until further use.

3.6. Chondrocyte culture and construct preparation

To evaluate chondrogenesis, primary chondrocytes (passage 0) were expanded for ~14 days (seeding density of $5*10^3$ cells/cm^2) in monolayer culture with chondrocyte expansion medium, consisting of DMEM (61965, Sigma Aldrich), 10% heat-inactivated FBS (Biowhittaker), 2.5% HEPES buffer solution (1M, final concentration 25mM, 15630, Gibco), pen/strep, and 10 ng/ml FGF-2 (R&D Systems, Abingdon, UK). Cells were trypsinized and used when they reached a confluence of 80-90%.

Equine chondrocytes (3 donors, passage 1) were resuspended in the different gelMA/gellan polymer solutions at 37°C, with a cell density of $10-20*10^6$ cells/ml (differences in cell density were between cell donors; for each donor, all hydrogel formulations were prepared with the same cell density). Exceptions were the 20% gelMA and 10/1% gelMA/gellan groups, which were mixed with the cells at 40°C since thermo-gelation occurred at 37°C. Cell laden hydrogels were cast in rectangular custom-made Teflon molds with a glass microscope slide on top and cross-linked by exposure to UV light as described above. After cross-linking, the hydrogel strips were cut into pieces of ca. 4 x 4 x 2 mm. The separate pieces were cultured in chondrogenic differentiation medium consisting of DMEM with 0.4 mM ascorbic acid (A8960, Sigma Aldrich), 1% Insulin-Transferrin-Selenium-X (31500, Gibco), 2.5% HEPES buffer solution (1M, final concentration 25mM, Gibco), 2% human serum albumin (Albuman 200g/L, final concentration 4g/L, Sanquin, the Netherlands), pen/strep, and 5 ng/mL TGF-β2 (302-B2, R&D Systems). Culture medium was refreshed twice a week and three samples for each gel formulation were harvested per cell donor at days 0, 14, 28, and 42.

3.7 Evaluation of chondrogenesis

3.7.1. Histology & Immunohistochemistry

At days 0, 14, 28, and 42, the cell-laden samples were harvested and half of each sample was fixed in formalin, dehydrated through a graded ethanol series, cleared in xylene and embedded in paraffin. Subsequently, 10 µm thick sections were cut from the embedded samples. Sections were stained with safranin-O to visualize glycosaminoglycans (GAGs), fast green to visualize collagen, and hematoxylin to stain cell nuclei[30].

Immunohistochemistry was used to visualize collagen type II distribution. Samples were deparaffinized with xylene and hydrated through graded ethanol series. After blocking for 10 minutes with H_2O_2 (0.3% in PBS), antigens were retrieved with pronase (1 mg/ml PBS, Roche life science, 11459643001, Indiana, USA) and hyaluronidase (10 mg/ml PBS, H2126, Sigma Aldrich) for 30 minutes at 37°C each. The primary antibody (DSHB, II-II6B3, dilution 1/100) was incubated overnight at 4°C. Mouse IgG (DAKO, X0931, same dilution as the primary antibody) was used as a negative control. The sections were incubated with the secondary antibody (final concentration: 1 µg/ml, IgG HRP, DAKO, P0447) for 60 minutes at room temperature. Next, the staining was developed with DAB peroxidase substrate solution (Sigma Aldrich) for 5-10 minutes. Counterstaining was performed with Mayer's Hematoxylin and after dehydration and clearing with xylene, the sections were mounted with DPX (100579, Merck Millipore, Billerica, MA, USA). All stained sections were evaluated and photographed using a light microscope (Olympus BX51 microscope, Olympus DP70 camera, Hamburg, Germany).

3.7.3. Biochemical assays

The remaining halves of the harvested cell-laden hydrogels were used for biochemical analysis. The samples were weighted (wet weight), freeze dried overnight and weighed again (dry weight). To determine the GAG and DNA contents, the samples were digested overnight at 56°C in 200 µL papain digestion buffer (0.2 M NaH_2PO_4 + 0.01 M EDTA*2 H_2O in milliQ, pH = 6.0) supplemented with 250 µL/mL papain solution (16-40 units/mg protein, P3125, Sigma Aldrich) and 0.01 M cysteine (C9768, Sigma Aldrich). The amount of sulfated GAGs, as a measure of proteoglycans, was determined with a dimethylmethylene blue (DMMB, pH = 3.0) assay[31] using known concentrations of chondroitin sulfate C (Sigma Aldrich) as a reference. In short, samples were diluted in PBS-EDTA and mixed with the DMMB solution. Excitation was measured directly after mixing at 525 nm and 595 nm with a versa max plate reader (Molecular devices, Wokingham, UK). The measurement at 525 nm was divided by the measurement at 595 nm and the GAG concentration of the samples was calculated from a quadratic fit of the standard curve and were corrected for the dilution. Quantification of DNA was

performed with a Quant-iT PicoGreen dsDNA kit (Molecular Probes, Invitrogen) using a spectrofluorometer (Biorad, Veenendaal, the Netherlands).

3.8. Statistics

Statistical analyses were performed using SPSS software (version 20, IBM Corporation, USA). The Young's moduli of the different gelMA/gellan concentrations were compared with a one-way ANOVA. To compare GAG production normalized to DNA in the different chondrocyte laden hydrogels per time point, a Randomized Block Design ANOVA was used (to correct for donor variability). The same test was used to compare DNA content normalized to the sample wet weight at the different time points per hydrogel formulation. For all tests, normality and homogeneity were assumed and, when significant differences were detected (significance level of 0.05), a Bonferroni post-hoc test was performed.

4. Results

4.1. Hydrogel filament screening

Multiple gelMA/gellan concentrations were evaluated for their ability to form a filament at cell-friendly temperatures (15-37°C). A well-defined filament of gelMA could be printed with a concentration of 7.5% w/v or higher, but only at specific, precise temperatures (Figure 3). By adding small amounts of gellan gum (0.5-1%) the minimally required gelMA concentration for filament formation could be reduced to 3% w/v and defined filaments could be formed at a wider temperature range compared to gelMA only solutions. The lowest evaluated polymer concentrations formed droplets at the nozzle and were, therefore, not considered suitable for printing. Additionally, it was investigated whether a cell pellet could be resuspended at 37°C. Hydrogels with the highest evaluated total polymer concentrations gelled at or above 37°C, disallowing the suspension of a cell pellet. Hydrogel compositions that met both criteria of forming defined filaments at a temperature in the range of 15-37°C, and being sufficiently fluid at 37°C to allow cell encapsulation, define the bioprinting window (red outline in Figure 3). With these formulations, 3D constructs with high shape fidelity could be printed (Figure 3B-D).
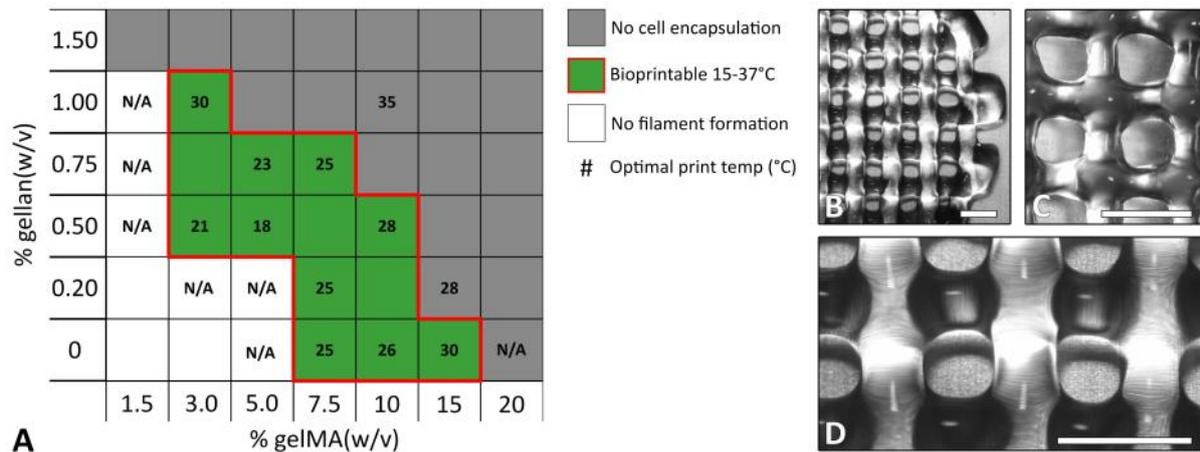
Fig. 3. *The bioprinting window for gelMA and gellan gum hydrogels (bordered by red line) and examples for printed constructs. A) Low polymer concentrations were too fluid to form a defined filament at 15 - 37°C (white), while high polymer concentrations formed too strong physical gels at 37°C to allow mixing with cells (dark grey). The middle range of polymer concentrations was suitable for bioprinting (green) although different optimal print temperatures were found (numbers in °C, for some formulations no optimal (cell-friendly) temperature could be found (N/A)). B) Image of a 3/1% gelMA/gellan construct printed at 30°C. C) Image of a 10/0.5% gelMA/gellan construct printed at 28°C. D) magnification of figure B. Scale bars represent 2 mm.*

Stress ramps were performed for a selected number of gelMA/gellan hydrogels (3/0.2%, 3/0.5%, 10/0% and 10/0.5%) at the observed optimal temperature for filament deposition or at 15°C for 3/0.2% gelMA/gellan, which did not form a filament between 15-37°C. All evaluated formulations showed a decrease in viscosity with increasing shear rate (Figure 4A). The yield stress, defined as the minimal stress necessary to induce flow in the polymer solution, was found to strongly correlate to the gellan gum concentration and was further increased by increasing the amount of gelMA (Figure 4B). The 3/0.2% gelMA/gellan formulation showed a gradual decrease in viscosity with increasing stress. A slightly steeper curve was observed for the 3/0.5% gelMA/gellan formulation and an even steeper curve was observed for the 10% gelMA formulation. An almost vertical curve was observed for the 10/0.5% gelMA/gellan formulation. For all measured formulations the viscosity drop (over the first decade of stress) after the yield point was calculated and was found to be largest for the formulation with 0.5% gellan gum. Finally, the yield stress and viscosity were measured at 37°C for 5/0.75%, 5/1%, 10/0.5% and 10/0.75% gelMA/gellan hydrogels to investigate what determined the ability to mix in cells (Figure 5). No difference in viscosity was observed between the groups, however, the yield stress and correlated viscosity was lower for 5/0.75% and 10/0.5% gelMA/gellan hydrogels compared to 5/1% and 10/0.75% gelMA/gellan formulations, which agreed with qualitative observations on the ability to resuspend cells in the hydrogels.

Formulation		Temp. (°C)	Yield stress (Pa)	Viscosity drop (Pa.s)
% gelMA (w/v)	% gellan (w/v)			
3	0.2	15	0.22±0.07	18.7±15.0
3	0.5	21	1.38±0.42	87.7±58.8
10	0	26	0.13±0.00	0.07±0.01
10	0.5	28	48.2±3.02	6583±880

Legend:
- – · – 3/0.2% gelMA/gellan, 15°C
- ····· 3/0.5% gelMA/gellan, 21°C
- – – 10% gelMA, 26°C
- —— 10/0.5% gelMA/gellan, 28°C
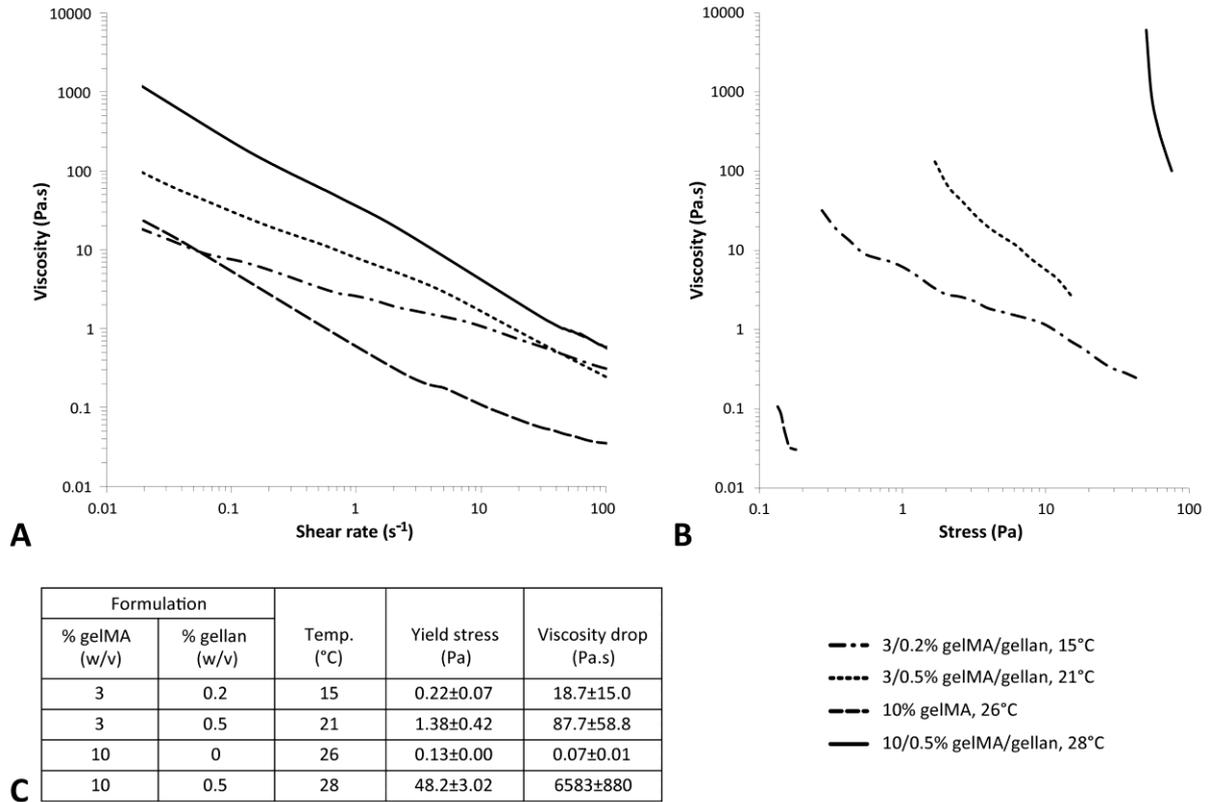
Fig. 4. Rheological measurements to support filament printing observations. The viscosity decreased for increasing shear ratse for all formulations (A). Yield stress and corresponding viscosity drop differed between formulations (B, C). Measurements were performed at the optimal bioprinting temperatures or at 15°C when no filament could be printed (C). Please note the logarithmic axes and that the viscosity drop was measured over 1 decade of stress starting from the yield stress, except for 10% gelMA which reached a plateau before one decade difference.
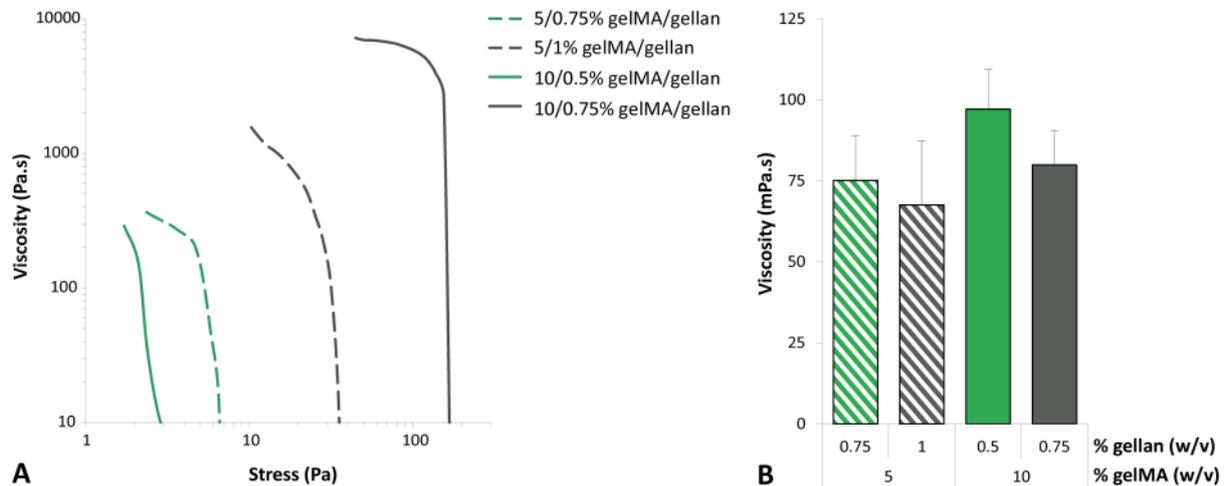
Fig. 5. Quantitation of rheological parameters that determine the ability to mix in cells. In green the formulations inside the bioprinting window and in grey the corresponding formulations above the bioprinting window. Yield stress and initial viscosity were relatively high for the formulation in which no cells could be resuspended (grey lines in A) while the viscosity, in flow, was similar for all the formulations (B, shear rate = 300/s). All measurements were performed at 37°C. Please note the logarithmic scales in figure A.

4.2. Mechanical evaluation

The Young's moduli were determined for multiple gelMA/gellan concentrations in unconfined compression. For each concentration, cell-free constructs were measured at equilibrium swelling on day 1 (Figure 6). Young's moduli varied between the different groups in a range of 2.7-186 kPa. Three smaller ranges in Young's moduli could be determined; 3/0.5%, 5/0.5% gelMA/gellan and 7.5% gelMA hydrogels had Young's moduli between 10-20 kPa, 3/1%, 5/0.75%, 1.5/0.75% gelMA/gellan and 10% gelMA formulations exhibited Young's moduli between 20-30 kPa and hydrogel formulations with higher total polymer concentrations showed Young's moduli in a range of 40-186 kPa.

Formulation		Young's modulus (kPa)	
% gelMA (w/v)	% gellan (w/v)		
3	0.5	12.8±1.0	
	1.0	23.3±1.8	
5	-	2.7±0.1	(#)
	0.5	16.3±0.6	
	0.75	26.9±1.6	
7.5	-	12.3±1.1	
	0.75	26.1±1.6	
10	-	24.1±4.3	
	0.5	47.2±4.1	($)
	1.0	77.8±6.4	($)
15	-	102.5±6.2	($)
20	-	186.0±19.2	($)
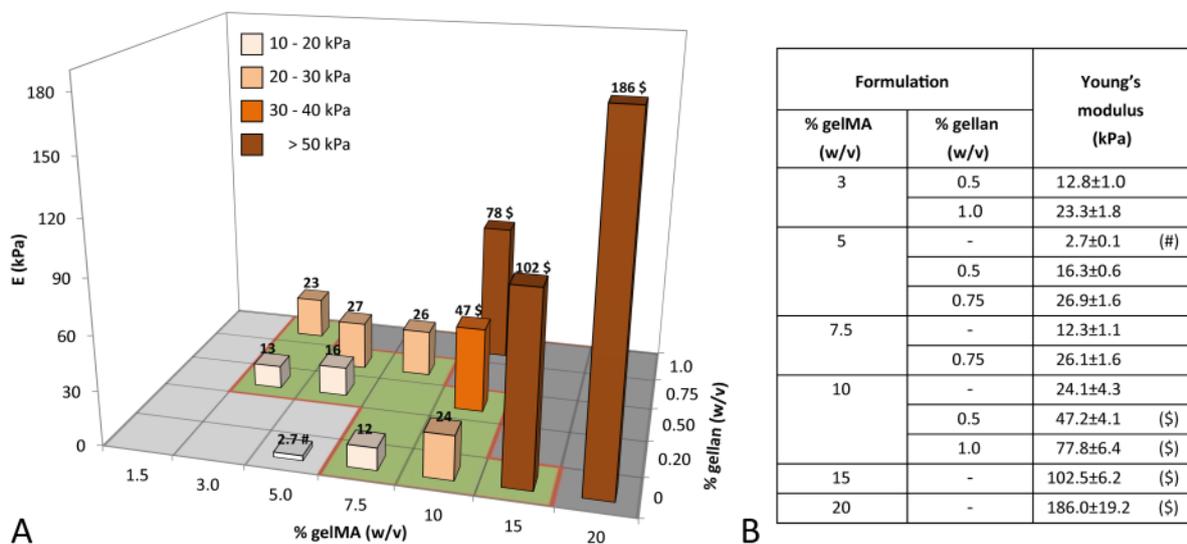
Fig. 6. *A grafical representation (A) and the absolute values (B) of the compressive Young's moduli (kPa) of UV cross-linked hydrogels for all evaluated concentrations. (#) Significantly different from the Young's modulus of 3/1%, 5/0.75%, 7.5/0.75% gelMA/gellan and 10% gelMA. ($) Significantly different from all other groups.*

4.3. Matrix production and accumulation

All gelMA/gellan formulations that were evaluated for supporting chondrogenesis allowed the deposition of cartilaginous matrix by the embedded chondrocytes. For samples from all formulations, the presence of GAGs was confirmed by safranin-O staining after 28 days of culture (data not shown). This staining was more intense and more homogeneous in the samples of day 42 (Figure 7). A similar pattern was found for the deposition of collagen type II. The distribution of cell-secreted matrix varied, depending on the polymer concentrations. Safranin-O and collagen type II stainings revealed homogeneous matrix deposition in the samples with low total polymer concentrations (3-10% gelMA with 0-1% gellan), while matrix clusters were visible around the cells in the 20% gelMA constructs and to a lesser extent in the 10/1% gelMA/gellan constructs.

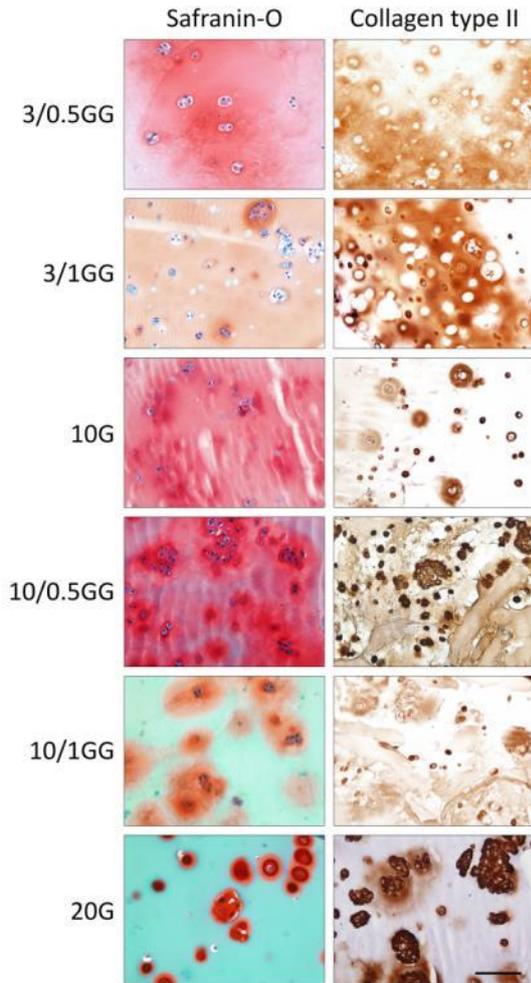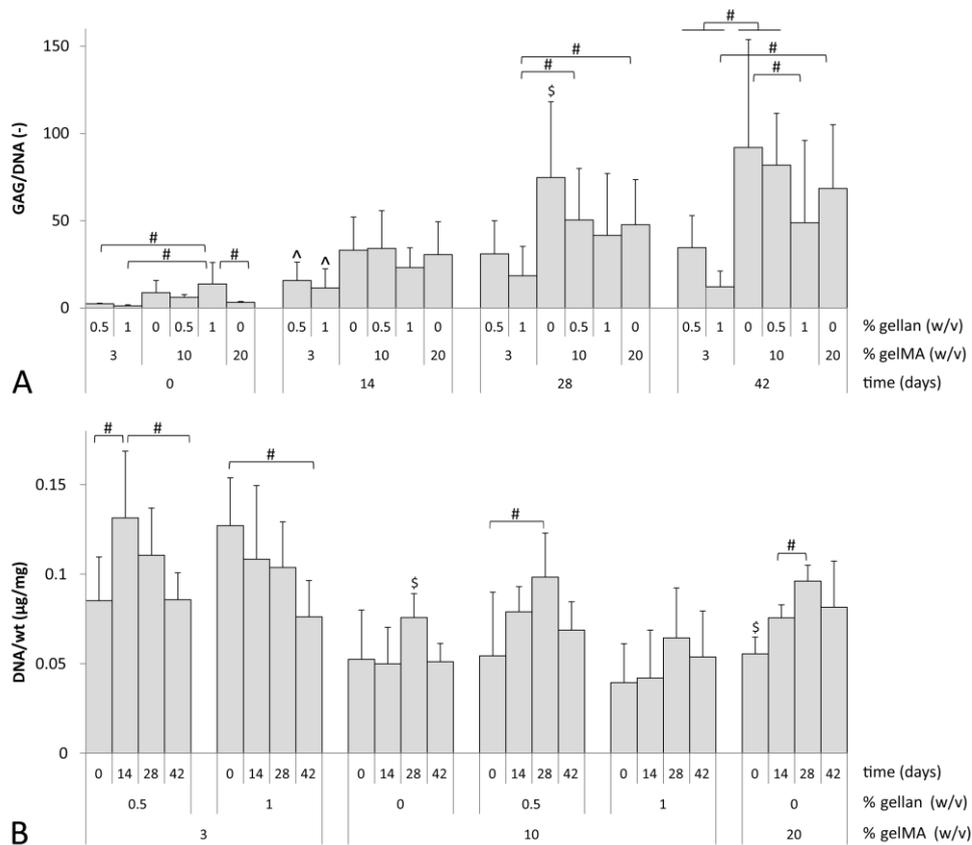***Fig. 7.*** *Extracellular cartilage matrix production after 42 days of differentiation culture. All hydrogel formulations supported GAG (column 1, in red) and collagen type II (column 2, in brown) formation of chondrocytes. Scale bar represents 100 µm for all images, G = gelMA, GG = gelMA/gellan. As gelMA is generated from denatured collagens it stains green with the Fast Green staining.*

For all cultured formulations, quantitative GAG and DNA measurements were performed at days 0, 14, 28 and 42 (Figure 8). All hydrogel formulations showed an increase in GAG/DNA content during the culture period. However, after 14 days of culture the 3/0.5% and 3/1% gelMA/gellan groups had significantly lower GAG/DNA values than the other hydrogel formulations. This trend remained visible during the final weeks of culture. At day 28, significantly higher GAG/DNA values were measured in 10% gelMA gels compared to all other groups. However, after 42 days of culture no significant differences were observed between the 10% gelMA, 10/0.5% gelMA/gellan and 20% gelMA groups. GAG normalized to the sample's wet weight showed an increase over time for all hydrogel formulations (data not shown). DNA normalized to the sample's wet weight showed a significant decrease over time for the 3/1% gelMA/gellan samples. The 3/0.5% gelMA/gellan hydrogels showed an increase in the first 14 days of culture and a decrease in the remaining culture period, while the DNA content increased during the first 28 days of culture in the 10% and 20% gelMA and 10/0.5% gelMA/gellan hydrogels. In the 10/1% gelMA/gellan hydrogels, no significant change in DNA per wet weight was observed over time.

Fig. 8. *GAG and DNA content for all hydrogel formulations at days 0, 14, 28 and 42 of differentiation culture. A) For all groups GAG normalized to DNA increased during the culture period. Highest levels were reached in the 10% gelMA and 10/0.5% gelMA/gellan hydrogels. B) DNA content normalized to the sample's wet weight (wt) decreased for the 3/0.5% and 3/1% gelMA/gellan hydrogels during culture. The other hydrogels showed an increase of DNA during the culture period. #) significant difference between both indicated groups (p<0.05), ^) significantly different from all other groups at the time point but equal to each other, $) significantly different from all other groups at that time point (A) or gel formulation (B).*

5. Discussion

The findings of this study reveal the bioprinting window of gelMA/gellan hydrogel blends. The lowest evaluated total polymer concentrations were too fluid for filament deposition and formed droplets at the printer nozzle, while the highest evaluated concentrations formed physical gels that appeared too solid to allow cell incorporation at 37°C. The bioprinting window of gelMA/gellan is defined as the intermediate area, in which both requirements of filament formation and miscibility with cells are met.

Although all evaluated gelMA/gellan compositions within the bioprinting window met both requirements and thus are suitable for bioprinting, different compositions possessed different material properties. Polymer solutions containing gellan gum allowed the deposition of filaments with less fine-tuning and optimization of print temperatures and printer settings, compared to their respective gelMA-only controls. This effect can be explained by the ionic crosslinks that gellan gum forms with gelMA and itself, which induce pseudo-plastic behavior (a form of shear thinning)[28] and an increase in yield stress, whereas gelMA-only gels rely mostly on thermal gelation to occur during and

directly after deposition[12,28]. Indeed, increased shear rate significantly reduced the viscosity for all evaluated formations. Even the 3/0.2% gelMA/gellan formulation, which could not form filaments at the nozzle of the bioprinter, showed shear thinning at 15°C. This demonstrates that shear thinning behavior is not the material property dictating filament formation and deposition. Instead, the polymer solutions that appeared printable within a broad range of conditions, exhibited relatively high yield stresses at the optimal print temperature (*e.g.* 48.2±3.0 Pa for 10/0.5% gelMA/gellan gum). At this stress, the yielding of the polymer solutions resulted in a steep viscosity drop (*e.g.* by 6.58±0.88 kPa·s for 10/0.5% gelMA/gellan). In contrast, the polymer solutions that could not form a filament within the 15-37°C range (*e.g.* 3/0.2% gelMA/gellan) did not exhibit clear yield behavior. These findings demonstrate that high yield stresses at which the viscosity reduces rapidly result in high printability of the polymer solution.

To better understand the upper boundary of the bioprinting window, two formulations below the boundary (5/0.75% and 10/0.5% gelMA/gellan) and the two corresponding concentrations above the boundary (5/1% and 10/0.75% gelMA/gellan) were evaluated for their viscosity and yield stress. Strikingly, the viscosity, when measured in flow, was the same for all four hydrogel formulations. Additionally, the measured values were within the range of previously reported viscosities for 10% gelMA and 20% gelMA polymer solutions[12]. However, the yield stresses and initial viscosities were higher in the formulations above the bioprinting window compared to their corresponding formulation in the bioprinting window. This implies that in gelMA/gellan blends, it is not the viscosity of the polymer solution that limits the miscibility with cells. Instead, the miscibility thus depends on the strength of the physical gel, which must be overcome in order to pipette the polymer solution. The transition from a gelMA/gellan formulation that can be mixed with a cell pellet to a formulation that cannot be mixed, lies in the yield stress range of 2-10 Pa.

This role of yield stress on the printability (filament formation and deposition) and miscibility with cells of a hydrogel has rarely been acknowledged in literature. Usually other rheological properties such as viscosity and shear thinning are stated as the most important parameters governing printability, while the viscosity is stated as the limiting factor for miscibility with cells[1,2,4,26,32–38]. Our observations demonstrate a crucial role of yield stress in both cell miscibility and filament formation and deposition. We highly recommend evaluating yield behavior in future bio-ink research and development, which will validate the universality of our observations for other gel systems.

The addition of gellan gum increased the stiffness of UV cured constructs. By changing the concentrations of gelMA and/or gellan gum, the construct stiffness could be tailored over a range from 2.7-186 kPa. The stiffness depended more strongly on the gellan gum concentration than on that of gelMA. Adding only 1% gellan gum to any of the evaluated gelMA concentrations, increased the Young's modulus with approximately ~30-40 kPa. By varying the gelMA and gellan concentrations, constructs with similar Young's moduli but with different compositions could be generated. The stiffest hydrogel constructs within the bioprinting window contained 15% gelMA and had a stiffness of 102.5±6.2 kPa. Even stiffer hydrogel constructs could be generated (*e.g.* 186.0±19.2 kPa for 20% gelMA). However, these hydrogels are not suitable for the incorporation of cells but may have other potential applications.

Besides gellan gum also hyaluronic acid is a viscosity enhancer that has been applied in bioprinting[10,39]. Similar increases in Young's moduli were observed for 10% gelMA hydrogels supplemented with hyaluronic acid as obtained in the current study with the gellan gum[25,40]. Although significant increases in the construct stiffness can be achieved with the addition of gellan gum, this is obviously not within the range of the reported stiffness of native cartilage, *i.e.* 400 − 800 kPa[41–43]. In addition, cell encapsulation in a hydrogel system is known to reduce the initial construct stiffness, dependent on the cell number[44,45]. This can be explained by the decrease in absolute polymer content per construct, due to the additional volume of the cells. Also the cells might interfere with the polymer network formation via physical hindrance. In order to create hydrogel-based load-bearing cartilage constructs additional strategies are required, such as *in vitro* pre-culture. It is well known that construct stiffness significantly increases when matrix is deposited by embedded cells[40,46–48]. Secondly, hydrogels can be reinforced with printed[49,50] or electrospun[51] thermoplastic polymers to increase their stiffness.

This study shows that all evaluated gelMA/gellan hydrogels support cartilage matrix production by embedded equine chondrocytes. However, the quantity and localization of the matrix production differed considerably between the various polymer blends. An important factor that can influence cell behavior is the stiffness of the surrounding matrix[52,53]. However, no clear correlation between cell performance and construct stiffness was found for this hydrogel system. Chondrocytes were cultured inside constructs with a Young's modulus ranging from 13 to 186 kPa. The softest constructs with a stiffness 13 and 23 kPa (3/0.5% gelMA/gellan and 3/1% gelMA/gellan, respectively) contained significantly less GAG/DNA compared to the stiffer constructs with a stiffness ranging from 24-186 kPa. In addition, considerable differences in matrix production and DNA content were found between gel formulations with similar Young's moduli. For example, significantly more GAG/DNA was

present in the 10% gelMA constructs compared to the 3/1% gelMA/gellan constructs while both have a Young's modulus of 23-24 kPa.

Hydrogel constructs with relatively high gellan gum concentrations (≥ 9% of the total polymer concentration) exhibited a decreased overall GAG production and the lowest proliferation rates. As previous studies showed excellent viability and cartilage-like matrix deposition by chondrocytes in hydrogels consisting of 0.7-5% gellan gum *in vitro* and *in vivo*[29,54,55], a toxic effect of the gellan gum appears to be unlikely. The presence of gellan gum, however, may inhibit the supportive effect that gelMA has on the matrix production of embedded cells. GelMA, which is produced from denatured collagens, stimulates chondrocytes in producing cartilage-like matrix[20,56–58]. The presence of relatively high gellan gum concentrations could inhibit this stimulatory effect. Likely, the cell performance is influenced by an interplay of the availability of cell adhesion sites and the mechanical environment[59,60].

In general, high polymer concentrations can inhibit matrix formation of embedded cells[7,8,61]. This was, however not found for the concentrations evaluated in the present study. Chondrocytes in the hydrogels with the lowest total polymer concentrations (3/0.5% gelMA/gellan and 3/1% gelMA/gellan) produced the least cartilage-like matrix and showed lower DNA content compared to hydrogels with higher total polymer concentrations. This is in contradiction to the study of Schuh *et al.* (2011)[62] who observed a negative effect of high polymer concentrations for cultured porcine chondrocytes in 0.75% and 3.5% agarose. On the other hand, when calf chondrocytes were embedded in 10%, 20% or 30% poly(ethylene glycol)-based (PEG-based) hydrogels, no difference was found in GAG production. This underscores that the inhibitory effect of high polymer concentrations on matrix production, observed in other studies, may also depend on other hydrogel properties *e.g.* cell adhesion sites and local construct stiffness, than purely on the polymer concentration.

Although no quantitative inhibitory effect based on the total polymer concentration was found in this study, differences in matrix distribution were observed. The newly formed matrix in hydrogel constructs with relatively high total polymer concentrations (≥ 11%) was confined in pericellular regions. Contrarily, newly formed matrix in hydrogel constructs with lower total polymer concentrations was evenly distributed after 42 days of culture. This suggests that high total polymer concentrations not necessarily inhibit matrix formation of chondrocytes, but do hamper the distribution of the newly formed matrix. This phenomenon was, for example, also observed in PEG[8]- and agarose[63]-based hydrogels. For an adequate increase in construct stiffness due to matrix production of embedded cells, the formation of a homogeneous interconnected tissue is required. Although the addition of gellan gum to gelMA hydrogels increased the initial construct stiffness with limited increase in the total polymer concentration, the maximum initial stiffness is restricted by the

homogeneous matrix deposition and the bioprinting requirements (≤47.2±4.1, 10/0.5% gelMA/gellan).

6. Conclusions

The bioprinting window for gelMA/gellan hydrogels was determined, designating a range of hydrogel compositions that allow printing of defined structures with encapsulated cells. This study showed that the addition of gellan gum to gelMA hydrogels (1) improves filament formation and deposition by inducing yielding behavior, (2) increases the overall construct stiffness, and (3) supports matrix production of embedded chondrocytes. However, too high yield stresses hinder cell incorporation, while relatively high gellan gum concentrations compromise cartilage matrix production of embedded chondrocytes. Additionally, high total polymer concentrations hamper the distribution of newly formed matrix. Of the studied hydrogel compositions, 10/0.5% gelMA/gellan hydrogels seemed most suited for the generation of chondrocyte-laden 3D printed cartilage equivalents. This formulation is relatively easy to process (printing and incorporating cells), and cross-linked hydrogel constructs have an appreciable Young's modulus of 47.2±4.1 kPa, while supporting cartilage tissue formation by chondrocytes and allowing for homogeneous matrix deposition. A generic requirement for filament formation appeared to be the combination of high yield stress with a large viscosity drop. However, yield stress also affected cell miscibility for gelMA/gellan hydrogels. This critical yield stress dependence may have important implications for future bio-ink development.

8. Reference

1.   Murphy, S. V & Atala, A. 3D bioprinting of tissues and organs. *Nat. Biotechnol.* **32,** 773–785 (2014).

2.   Malda, J. *et al.* 25th anniversary article: Engineering hydrogels for biofabrication. *Adv. Mater.* **25,** 5011–28 (2013).

3.   Zhao, G., Zhang, X., Lu, T. J. & Xu, F. Recent Advances in Electrospun Nanofibrous Scaffolds for Cardiac Tissue Engineering. *Adv. Funct. Mater.* **25,** 5726–5738 (2015).

4.   Jungst, T., Smolan, W., Schacht, K., Scheibel, T. & Groll, J. Strategies and Molecular Design Criteria for 3D Printable Hydrogels. *Chem. Rev.* **116,** 1496–1539 (2016).

5.   Gao, B. *et al.* 4D Bioprinting for Biomedical Applications. *Trends Biotechnol.* **xx,** 1–11 (2016).

6.   Møller, P. C. F., Fall, A. & Bonn, D. Origin of apparent viscosity in yield stress fluids below yielding. *EPL (Europhysics Lett.)* **87,** 38004 (2009).

7.   Seliktar, D. Designing cell-compatible hydrogels for biomedical applications. *Science* **336,** 1124–8 (2012).

8.   Bryant, S. J. & Anseth, K. S. Hydrogel properties influence ECM production by chondrocytes photoencapsulated in poly (ethylene glycol) hydrogels. *J. Biomed. Mater. Res.* **59,** 63–71 (2001).

9.   Smith, C. M. *et al.* Three-dimensional bioassembly tool for generating viable tissue-engineered constructs. *Tissue Eng.* **10,** 1566–1576 (2004).

10.   Schuurman, W. *et al.* Gelatin-methacrylamide hydrogels as potential biomaterials for fabrication of tissue-engineered cartilage constructs. *Macromol. Biosci.* **13,** 551–561 (2013).

11.   Visser, J. *et al.* Biofabrication of multi-material anatomically shaped tissue constructs. *Biofabrication* **5,** 035007 (2013).

12.   Billiet, T., Gevaert, E., De Schryver, T., Cornelissen, M. & Dubruel, P. The 3D printing of gelatin methacrylamide cell-laden tissue-engineered constructs with high cell viability. *Biomaterials* **35,** 49–62 (2014).

13.   Skardal, A. *et al.* Photocrosslinkable hyaluronan-gelatin hydrogels for two-step bioprinting. *Tissue Eng. Part A* **16,** 2675–85 (2010).

14.   Yan, Y. *et al.* Fabrication of viable tissue-engineered constructs with 3D cell-assembly technique. *Biomaterials* **26,** 5864–71 (2005).

15.   Cohen, D. L., Malone, E., Lipson, H. & Bonassar, L. J. Direct freeform fabrication of seeded hydrogels in arbitrary geometries. *Tissue Eng.* **12,** 1325–1335 (2006).

16.   Fedorovich, N. E. *et al.* Evaluation of photocrosslinked Lutrol hydrogel for tissue printing applications. *Biomacromolecules* **10,** 1689–96 (2009).

17.   Pescosolido, L. *et al.* Hyaluronic acid and dextran-based semi-IPN hydrogels as biomaterials for bioprinting. *Biomacromolecules* **12,** 1831–1838 (2011).

18.   Censi, R. *et al.* A Printable Photopolymerizable Thermosensitive p(HPMAm-lactate)-PEG Hydrogel for Tissue Engineering. *Adv. Funct. Mater.* **21,** 1833–1842 (2011).

19.   Dang, J. M. & Leong, K. W. Natural polymers for gene delivery and tissue engineering. *Adv. Drug Deliv. Rev.* **58,** 487–99 (2006).

20.   Nichol, J. W. *et al.* Cell-laden microengineered gelatin methacrylate hydrogels. *Biomaterials* **31,** 5536–44 (2010).

21.   Van Den Bulcke, A. I. *et al.* Structural and Rheological Properties of Methacrylamide Modified Gelatin Hydrogels. *Biomacromolecules* **1,** 31–38 (2000).

22.   Almarza, A. J. & Athanasiou, K. A. Design characteristics for the tissue engineering of cartilaginous tissues. *Ann. Biomed. Eng.* **32,** 2–17 (2004).

23.   Prakash, D. & Learmonth, D. Natural progression of osteo-chondral defect in the femoral condyle. *Knee* **9,** 7–10 (2002).

24.   Klein, T. J. *et al.* Strategies for Zonal Cartilage Repair using Hydrogels. *Macromol. Biosci.* **9,** 1049–1058 (2009).

25.   Levett, P. A. *et al.* A biomimetic extracellular matrix for cartilage tissue engineering centered on photocurable gelatin, hyaluronic acid and chondroitin sulfate. *Acta Biomater.* **10,** 214–223 (2014).

26.   Yue, K. *et al.* Synthesis, properties, and biomedical applications of gelatin methacryloyl (GelMA) hydrogels. *Biomaterials* **73,** 254–271 (2015).

27.   Gao, G. *et al.* Improved properties of bone and cartilage tissue from 3D inkjet-bioprinted human mesenchymal stem cells by simultaneous deposition and photocrosslinking in PEG-GelMA. *Biotechnol. Lett.* **37,** 2349–2355 (2015).

28.   Melchels, F. P. W., Dhert, W. J. A., Hutmacher, D. W. & Malda, J. Development and characterisation of a new bioink for additive tissue manufacturing. *J. Mater. Chem. B* **2,** 2282–2289 (2014).

29.   Oliveira, J. T. *et al.* Injectable gellan gum hydrogels with autologous cells for the treatment of rabbit articular cartilage defects. *J. Orthop. Res.* **28,** 1193–9 (2010).

30.   Rosenberg, L. Chemical basis for the histological use of safranin O in the study of articular cartilage. *J. Bone Joint Surg. Am.* **53,** 69–82 (1971).

31.   Farndale, R. W., Sayers, C. A. & Barrett, A. J. A Direct Spectrophotometric Microassay for Sulfated Glycosaminoglycans in Cartilage Cultures. *Connect. Tissue Res.* **9,** 247–248 (1982).

32.   Schuurman, W. *et al.* Bioprinting of hybrid tissue constructs with tailorable mechanical properties. *Biofabrication* **3,** 021001 (2011).

33.   Xu, T. *et al.* Hybrid printing of mechanically and biologically improved constructs for cartilage tissue engineering applications. *Biofabrication* **5,** 015001 (2013).

34.   Zhao, Y., Li, Y., Mao, S., Sun, W. & Yao, R. The influence of printing parameters on cell survival rate and printability in microextrusion-based 3D cell printing technology. *Biofabrication* **7,** 045002 (2015).

35.   Hoch, E., Hirth, T., Tovar, G. E. M. & Borchers, K. Chemical tailoring of gelatin to adjust its chemical and physical properties for functional bioprinting. *J. Mater. Chem. B* **1,** 5675 (2013).

36.   Ozbolat, I. T. & Hospodiuk, M. Current advances and future perspectives in extrusion-based bioprinting. *Biomaterials* **76,** 321–343 (2016).

37.   Kesti, M. *et al.* Bioprinting Complex Cartilaginous Structures with Clinically Compliant Biomaterials. *Adv. Funct. Mater.* **25,** 7406–7417 (2015).

38.   Highley, C. B., Rodell, C. B. & Burdick, J. A. Direct 3D Printing of Shear-Thinning Hydrogels into Self-Healing Hydrogels. *Adv. Mater.* **27,** 5075–5079 (2015).

39.   Fam, H., Kontopoulou, M. & Bryant, J. T. Effect of concentration and molecular weight on the rheology of hyaluronic acid/bovine calf serum solutions. *Biorheology* **46,** 31–43 (2009).

40.   Levett, P. A., Hutmacher, D. W., Malda, J. & Klein, T. J. Hyaluronic acid enhances the mechanical properties of tissue-engineered cartilage constructs. *PLoS One* **9,** e113216 (2014).

41.   Chen, A. C., Bae, W. C., Schinagl, R. M. & Sah, R. L. Depth- and strain-dependent mechanical and electromechanical properties of full-thickness bovine articular cartilage in confined compression. *J. Biomech.* **34,** 1–12 (2001).

42.   Athanasiou, K. A., Agarwal, A. & Dzida, F. J. Comparative study of the intrinsic mechanical properties of the human acetabular and femoral head cartilage. *J. Orthop. Res.* **12,** 340–349 (1994).

43.   Jurvelin, J. S., Buschmann, M. D. & Hunziker, E. B. Optical and mechanical determination of poisson's ratio of adult bovine humeral articular cartilage. *J. Biomech.* **30,** 235–241 (1997).

44. Mauck, R. L., Wang, C. .-B., Oswald, E. S., Ateshian, G. A. & Hung, C. T. The role of cell seeding density and nutrient supply for articular cartilage tissue engineering with deformational loading. *Osteoarthr. Cartil.* **11,** 879–890 (2003).

45. Reza, A. T. & Nicoll, S. B. Characterization of novel photocrosslinked carboxymethylcellulose hydrogels for encapsulation of nucleus pulposus cells. *Acta Biomater.* **6,** 179–186 (2010).

46. Williams, G. M., Klein, T. J. & Sah, R. L. Cell density alters matrix accumulation in two distinct fractions and the mechanical integrity of alginate–chondrocyte constructs. *Acta Biomater.* **1,** 625–633 (2005).

47. Ng, K. W. *et al.* A layered agarose approach to fabricate depth-dependent inhomogeneity in chondrocyte-seeded constructs. *J. Orthop. Res.* **23,** 134–141 (2005).

48. Reza, A. T. & Nicoll, S. B. Characterization of novel photocrosslinked carboxymethylcellulose hydrogels for encapsulation of nucleus pulposus cells. *Acta Biomater.* **6,** 179–186 (2010).

49. Schuurman, W. *et al.* Three-dimensional assembly of tissue-engineered cartilage constructs results in cartilaginous tissue formation without retainment of zonal characteristics. *J. Tissue Eng. Regen. Med.* n/a–n/a (2013). doi:10.1002/term.1726

50. Shim, J.-H., Kim, J. Y., Park, M., Park, J. & Cho, D.-W. Development of a hybrid scaffold with synthetic biomaterials and hydrogel using solid freeform fabrication technology. *Biofabrication* **3,** 034102 (2011).

51. Visser, J. *et al.* Reinforcement of hydrogels using three-dimensionally printed microfibres. *Nat. Commun.* **6,** 6933 (2015).

52. Discher, D. E., Janmey, P. & Wang, Y.-L. Tissue cells feel and respond to the stiffness of their substrate. *Science* **310,** 1139–1143 (2005).

53. Huang, G. *et al.* Engineering three-dimensional cell mechanical microenvironment with hydrogels. *Biofabrication* **4,** 042001 (2012).

54. Gong, Y. *et al.* An improved injectable polysaccharide hydrogel: modified gellan gum for long-term cartilage regeneration in vitro. *J. Mater. Chem.* **19,** 1968 (2009).

55. Oliveira, J. T. *et al.* Gellan gum: A new biomaterial for cartilage tissue engineering applications. *J. Biomed. Mater. Res. - Part A* **93,** 852–863 (2010).

56. Zhang, J., Mujeeb, A., Du, Y., Lin, J. & Ge, Z. Probing cell-matrix interactions in RGD-decorated macroporous poly (ethylene glycol) hydrogels for 3D chondrocyte culture. *Biomed. Mater.* **10,** 035016 (2015).

57.   Chen, J.-P. & Su, C.-H. Surface modification of electrospun PLLA nanofibers by plasma treatment and cationized gelatin immobilization for cartilage tissue engineering. *Acta Biomater.* **7,** 234–43 (2011).

58.   Lee, H. *et al.* Chondrocyte 3D-culture in RGD-modified crosslinked hydrogel with temperature-controllable modulus. *Macromol. Res.* **20,** 106–111 (2012).

59.   Trappmann, B. *et al.* Extracellular-matrix tethering regulates stem-cell fate. *Nat. Mater.* **11,** 742–742 (2012).

60.   Trappmann, B. & Chen, C. S. How cells sense extracellular matrix stiffness: A material's perspective. *Current Opinion in Biotechnology* **24,** 948–953 (2013).

61.   Schuh, E. *et al.* The influence of matrix elasticity on chondrocyte behavior in 3D. *J. Tissue Eng. Regen. Med.* **6,** e31–e42 (2012).

62.   Schuh, E. *et al.* Chondrocyte redifferentiation in 3D: the effect of adhesion site density and substrate elasticity. *J. Biomed. Mater. Res. A* **100,** 38–47 (2012).

63.   Kock, L. M., Geraedts, J., Ito, K. & van Donkelaar, C. C. Low Agarose Concentration and TGF-β3 Distribute Extracellular Matrix in Tissue-Engineered Cartilage. *Tissue Eng. Part A* **19,** 1621–1631 (2013).